Desalination and Water Treatment
www.deswater.com

doi: 10.1080/19443994.2015.1099470

57 (2016) 19357–19373
September

Taylor & Francis
Taylor & Francis Group

Comparative study on photocatalytic decolorization of an anionic and a cationic dye using different TiO_2 photocatalysts

Nassima Laid*, Nour Bouanimba, Razika Zouaghi, Tahar Sehili

Laboratoire des Sciences et Technologie de l'Environnement (LSTE), Faculté des Sciences Exactes, Département de Chimie, Université de Frères Mentouri Constantine, Algeria, Tel./Fax: +213 31 81 88 16; emails: laidns25@gmail.com (N. Laid), nourbouanimba@gmail.com (N. Bouanimba), razika_zouaghi@yahoo.fr (R. Zouaghi), tsehili@yahoo.fr (T. Sehili)

Received 30 November 2014; Accepted 14 September 2015

ABSTRACT

The photocatalytic degradation of Malachite green oxalate (MG), a cationic dye, and Eosin yellow (EY), an anionic dye, was studied and compared using different TiO_2 catalysts such as Degussa P25 and Millennium PC: PC500, PC105, PC100, and PC50 in slurry form under UV irradiation at natural, acidic, and alkaline mediums. The structural properties and phase composition of the TiO_2 samples were determined by X-ray diffractometry. The obtained results indicated that the photocatalytic activity was correlated to the crystalline phase and the particle sizes of each catalyst; the mixed phase of anatase/rutile (Degussa P25) exhibited a higher photoactivity to degrade both dyes than pure-phase anatase (Millennium PC). In addition, TiO_2 with larger particles and lower surface area (P25 and PC50) performed better in the degradation of both dyes in comparison with smaller particles and larger surface area. An enhancement of the degradation efficiency was observed in alkaline medium for the cationic dye (MG) and in acidic medium for the anionic dye (EY). In an acidic medium, the various degrees of rate degradation obtained using three different proton sources of pH (H_2SO_4, HCl, and $HClO_4$) are directly related to the presence of the corresponding counter ions. The effect of various parameters like the presence of Cl^-, HCO_3^-, and H_2O_2 on the photocatalytic degradation of both dyes, using Degussa P25 as photocatalyst, depends on several factors such as their concentrations in solution, pH, dye structure, and the previous adsorption in the dark.

Keywords: Photocatalysis; Adsorption; Dye; Titanium dioxide; H_2O_2; Inorganic salts

1. Introduction

The release of colored wastewaters in the ecosystem is a dramatic source of esthetic pollution, eutrophication, and perturbations in aquatic life. For the majority of them, their half-lives under sunlight are greater than 2,000 h [1] and their resistance to biological and even chemical degradation [2,3] makes them hazardous for the environment even at low concentrations.

Currently, chemical methods such as advanced oxidation processes (AOPs) seem to be more promising for the treatment of colored industrial effluents. AOPs were based on the generation of very reactive species such as hydroxyl radicals ($^{\cdot}OH$) that oxidize a broad range of pollutants quickly and none selectively. Among various AOPs, heterogeneous photocatalysis

---

*Corresponding author.

on metal oxide semiconductor particles has been found to be very effective for removing the organic pollutants from wastewater [4,5]. The key advantage of the former is its inherent destructive nature: it does not involve mass transfer [6]; it can be carried out under ambient conditions and may lead to complete mineralization of organic carbon into CO_2.

Among the semiconductors used, titanium dioxide (TiO_2) is considered a very efficient catalyst that, unlike other semiconductors, is nontoxic, stable to photocorrosion, low cost, and suitable to work using sunlight as energy source. Various research works have been carried out on dye wastewater purification by TiO_2 catalyst under UV irradiation [7–9]. The type of TiO_2 used plays an important role during the photocatalytic degradation of dye pollutants, since the rate of formation of oxidative radicals and the adsorption of pollutant on the TiO_2 surface are functions of the titania size, BET area, crystalline phase, uniformity, etc. [10]. To date, most work performed on the photocatalytic destruction of dyes by UV/TiO_2 process has been performed using Degussa P25. In addition to P25, there are a number of commercial available TiO_2 catalyst materials that could be used for dyes' destruction. TiO_2 from Millennium was less studied than Degussa P25; they are expected to be photocatalytically as efficient as P25, or more, since they are 100% anatase which is the active form of TiO_2, whereas P25 contains only 80% of this form. However, the majority of studies on TiO_2 reported that P25 appeared to be the most effective catalyst for the degradation of organic compounds such as benzenesulfonic acids [11], metobromuron [12], microcystin-LR [13] and methabenzthiazuron [14], although its surface area was lower than that of most of the Millennium TiO_2. However, few studies deal with the use of TiO_2 from Millennium for the photocatalytic degradation of dyes [15].

It is well known that for a photocatalytic process, adsorption properties of a photocatalyst play an important role during the degradation process and that the TiO_2 photodegradation occurs on or near the semiconductor surface [16]. Hence, greater the adsorption, higher is the rate of degradation. Adsorption of pollutant on the catalyst surface and the efficiency of the photocatalytic degradation are affected by several factors, which may include the type of catalyst, effluent composition, pH, and the type and charge of the degraded compound.

In the chemical classification method, dyes are grouped according to certain common chemical structural features. Cationic and anionic dyes are the two main groups. It was found that in photocatalytic degradation, the adsorption level on TiO_2 is higher for dyes with a positive charge (cationic) than for those with a negative charge (anionic) [8]. This result was explicated by the ability of the degraded compound to be adsorbed on the surface of the catalyst.

The present study is primarily concerned with the photocatalytic degradation of Malachite green oxalate (MG), a cationic triphenylmethane dye and Eosin yellow (EY), an anionic xanthene dye, by a series of titania samples from Degussa (P25) and Millennium (PC500, PC105, PC100, PC50). Both the investigated dyes are extensively used in the textile, paper, and leather industries and medicines. Both are hazardous compounds [17,18] and suspected to be toxic and carcinogen for humans and animals [19,20]. The principal objective of this investigation is to determine the effect of the charge of the degraded compound, the type, and the phase structure of TiO_2, and the pH of solution for the degradation efficiency. This study is also expected to improve the understanding of the relationship between the photocatalytic degradation reaction and the adsorption phenomenon of dyes on the catalysts surface, at different pH conditions.

2. Experimental methods

2.1. Materials

Malachite green oxalate (MG) (C.I. 42000, molecular formula: $C_{52}H_{54}N_4O_{12}$, molecular weight 927.01 g moL^{-1}) and EY (C.I. 45380, molecular formula: $C_{20}H_6Br_4Na_2O_5$, molecular weight 691.86 g moL^{-1}) were supplied by Merck reactifs. Their molecular structures are given in Table 1.

The photocatalyst Degussa P25 was used for the degradation of MG and EY in most of the experiments. Other photocatalyst powders namely, TiO_2 Millennium PC50, PC100, PC105, and PC500 were used for comparative study. The structural properties and phase composition of the TiO_2 samples were determined by X-ray diffractometry using a BRUKER ADVANCE D8 diffractometer with Cu ($\lambda = 1.5406$ Å) radiation. Results are illustrated in Fig. 1. The mean crystallite sizes of TiO_2 samples were evaluated using the Debye–Scherrer formula:

$$D\ (2\theta) = \frac{K\lambda}{\beta \cos \theta} \tag{1}$$

where D is the mean crystallite size (nm), K is the constant which is taken as 0.90, λ is the wavelength of the X-ray radiation, β is the reflection full-width at half maximum (FWHM), and θ is the diffraction angle.

The obtained X-ray diffraction patterns were compared with the standard anatase and rutile

Table 1
Structures and characteristics of Malachite green oxalate and Eosin yellow

Dye	Molecular formula	Molecular structure	λ_{max} (nm)
Eosin yellow (EY)	$C_{20}H_6Br_4Na_2O_5$	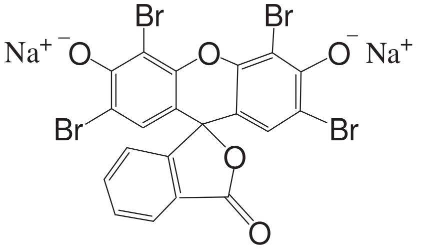	516
Malachite green oxalate (MG)	$C_{52}H_{54}N_4O_{12}$	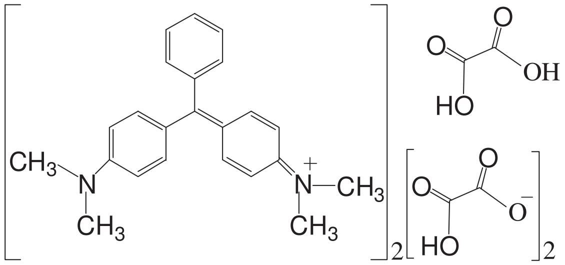	616

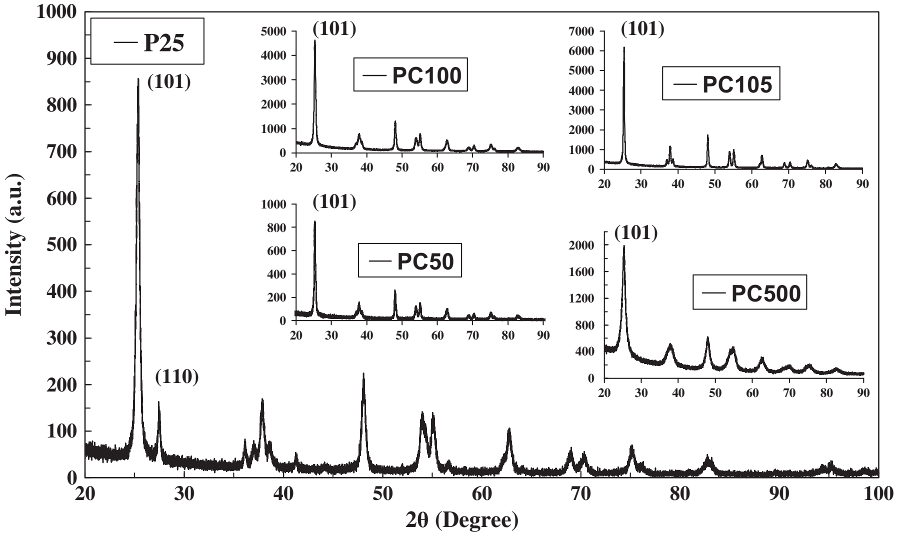

Fig. 1. X-ray diffraction pattern of all the samples.

diffractograms. The phase percentage formed was determined from the integrated intensity peak at $2\theta = 25.3^\circ$ (1 0 1) for anatase and $2\theta = 27.4^\circ$ (1 1 0) for rutile. The percentage of anatase, A, was determined using Eq. (2) [21]:

$$A\ (\%) = 100/(1 + 1.265 I_R/I_A) \qquad (2)$$

where I_R is the intensity of the rutile peak at $2\theta = 27.4^\circ$ and I_A is the intensity of the anatase peak at $2\theta = 25.3^\circ$.

The crystallite size, phase composition, and specific surface area of the TiO_2 samples are given in Table 2.

Water was purified by Milli-Q system (Millipore) and was used to prepare experimental solutions. The natural pH of the aqueous dyes solution is 6.8 and 5.8 for MG and EY, respectively. The pH of the solutions was adjusted using $HClO_4$, H_2SO_4, and HCl from Merck and NaOH from Carlo Erba. H_2O_2 and NaCl were purchased from Labosi and $NaHCO_3$ was purchased from Prolabo. The other chemicals used in this

Table 2
Chemical and physical properties of the photocatalysts

Catalyst	Composition (%) Anatase/rutile	Specific surface ($m^2 g^{-1}$)	Particle size (nm)
P25	80/20	55[a]	20
PC50	100	45 ± 5[a]	19
PC100	100	80–100[a]	16
PC105	100	75–95[a]	24
PC500	100	345[a]	8

[a] Provided by the particle manufacturer.

study such as $HgSO_4$, $K_2Cr_2O_7$, and Ag_2SO_4 were obtained from Sigma-Aldrich.

2.2. Procedure and analysis

The photocatalysis and adsorption experiments were carried out with 50 ml of solution with a desired dye concentration (10 mg L^{-1}) and TiO_2 loading (1 g L^{-1}) at natural pH and at a temperature of 20˚C; the slurry composed of dye solution and the catalyst was placed in the reactor and stirred magnetically to maintain TiO_2 in suspension. The suspension was left for 30 min in the dark in order to achieve the maximum adsorption of the dye onto the catalyst surface. The reaction vessel was fitted with four Philips HPW125 (UV-A, λ_{max} = 365 nm) low-pressure mercury UV lamps. During both dark adsorption and UV-irradiation periods, samples of 3 ml were taken out from the reaction mixture at regular time intervals and filtered on a Millipore filter prior to analysis and the absorbance was measured at λ_{max} = 616 nm and λ_{max} = 516 nm for MG and EY, respectively. A HELIOS α-UNICAM spectrophotometer was used for measuring absorbance at different time intervals.

In order to determine the extent of mineralization, samples were taken out at regular time intervals and the organic content was measured using a chemical oxygen demand (COD) analyzer. COD was measured according to the method presented by Thomas and Mazas [22] using a dichromate solution as the oxidizer in a strong acid medium. Test solution (2 mL) was transferred into the dichromate reagent and digested at 150˚C for 2 h. The optical density for the color change of dichromate solution was determined with a UV–vis spectrophotometer.

The efficiency of color removal and the dye mineralization were defined by the following equations:

$$\text{Decolorization } (\%) = \frac{\left([\text{Dye}]_0 - [\text{Dye}]_t\right)}{[\text{Dye}]_0} \times 100 \quad (3)$$

$$\text{Mineralization } (\%) = \frac{\left([\text{COD}]_0 - [\text{COD}]_t\right)}{[\text{COD}]_0} \times 100 \quad (4)$$

where $[\text{Dye}]_t$ and $[\text{Dye}]_0$ are the dye concentrations at time t and initial concentrations, respectively. $[\text{COD}]_t$ and $[\text{COD}]_0$ are the COD concentrations at time t and initial concentrations, respectively.

The amount of dye adsorbed onto the TiO_2 (mg g^{-1}) was calculated using the following equation:

$$Q_{\text{ads}} = \frac{(C_0 - C_t)V}{m} \quad (5)$$

where Q_{ads} is the adsorbed quantity at time t (mg g^{-1}), C_0 is the initial dye concentration (mg L^{-1}), C_t is the dye concentration (mg L^{-1}) at the moment t of the process of adsorption, V is the volume of the solution (L), and m is the weight of adsorbent (g).

3. Results and discussion

3.1. Kinetics of the photocatalytic degradation

The elimination of both dyes was studied at two different experimental conditions: (i) under UV illumination in the absence of TiO_2 (photolysis), (ii) under UV illumination in the presence of TiO_2 P25 (photocatalysis). Fig. 2 shows the kinetics disappearances of MG and EY by photolysis (UV) and photocatalysis (UV/TiO_2).

As can be seen, irradiation in the absence of P25 showed no significant decolorization. However, in the presence of P25, a rapid decolorization of MG and EY occurred by irradiation. This demonstrates that the photocatalytic experiments occurred in a pure photocatalytic regime where photochemical processes can be neglected.

The decrease in the dyes' concentration by the progress of photocatalysis means that $^{\cdot}OH$ radicals and other oxidant formed through photocatalysis

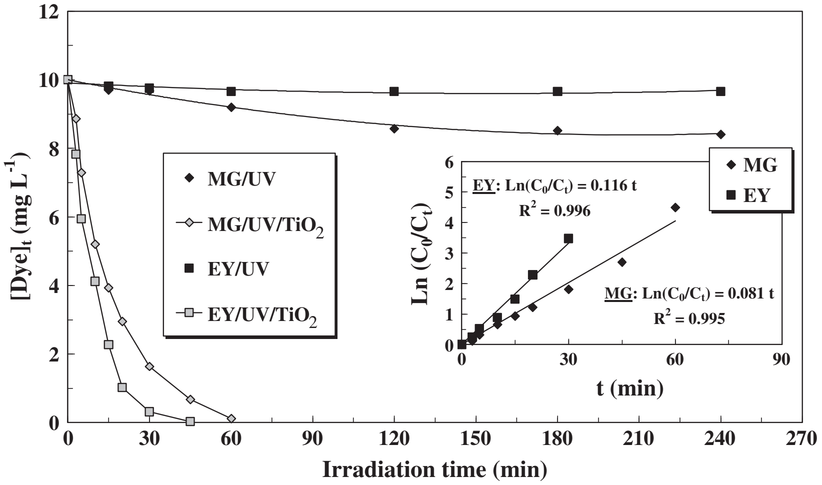

Fig. 2. Comparison of photolysis and photocatalytic degradation kinetics of MG and EY. In the inset: $\ln(C_0/C_t) = f(t)$: ([Dye] = 10 mg L^{-1}, [P25] = 1 g L^{-1}, I = 2.5 mW cm^{-2}, and at natural pH (6.3 ± 0.5)).

attacked the chromophores responsible for the characteristic color of the two dyes and diminished their colors. The removal of the anionic dye (EY) was obviously faster than the cationic dye (MG). This may be attributed to several factors. First, it may be due to the difference in chemical structure of the two dyes, resulting in difference in absorption characteristics and in susceptibility to photodegradation. MG has a more complex chemical structure, making it less photodegradable. The substituent groups have also an effect on the rate of photodegradation of both dyes; the presence of $–CH_3$ group in MG molecular structure can slightly decrease the reactivity of this dye [23]. Another reason explaining the fast degradation of EY may be because EY is an anionic dye and the natural pH of the aqueous dye solution of EY is 5.8. In this pH value, the surface charge of TiO_2 may be positive (pH_{pzc} = 6.8) and therefore, shows more tendencies to adsorb a negative species like EY leading to the highest effectiveness of this dye in adsorption and photocatalysis [24].

The degradation experiments by UV irradiation of dye aqueous solutions containing TiO_2 follow the pseudo-first-order kinetic law with respect to the concentration of the dye in the solution (inset in Fig. 2), according to the equation:

$$\ln\left(\frac{C_0}{C_t}\right) = k_{\mathrm{app}}t \tag{6}$$

where C_0 is the initial concentration of dye (mg L^{-1}), C_t is the instant concentration of dye in the sample at time t (mg L^{-1}), k_{app} is the pseudo-first-order reaction rate constant (min^{-1}), and t is the reaction time (min).

The degradation rate for both dyes was found to follow pseudo-first-order reaction kinetics and the degradation rate was calculated in terms of mg L^{-1} min^{-1}. The pseudo-first-order reaction rate constant calculated was 0.081 and 0.116 min^{-1} for MG and EY, respectively.

3.2. Kinetics of the total mineralization

COD indicates the extent of degradation or mineralization of organic matter. The kinetics of the total mineralization have been followed using the disappearance of the COD. All the experiments were carried out under the normal reaction conditions at an intensity of 2.5 mW cm^{-2}, aperture to volume ratio (A/V) of 0.14 cm^2 mL^{-1} of the reactor, dye concentration of 10 mg L^{-1}, catalyst loading of 1 g L^{-1}, and at a natural pH of the solutions (pH ≈ 6.3 ± 0.5); the results are shown in Fig. 3. The initial COD of MG and EY dyes was found to be 17.50 and 7.90 mg L^{-1}, respectively. After the adsorption equilibrium (30 min), the COD was found to be 13.47 and 5.79 mg L^{-1} for MG and EY, respectively. After five hours of the photocatalytic reaction, the final COD was found to be 4.25 and 0.64 mg L^{-1}, respectively. These results indicated that 76 and 92% of MG and EY were degraded in 5 h, respectively. Change in COD further confirms the degradation leading to decrease in the organic content. The anionic dye (EY) has the smallest COD, which is first eliminated because it has the smaller number of carbon atoms ($C_{20}H_6Br_4Na_2O_5$: n = 20) than the cationic dye (MG) ($C_{52}H_{54}N_4O_{12}$: n = 52). In addition, it is observed that the COD decreases slower than the decolorization of the solution for both dyes. Complete

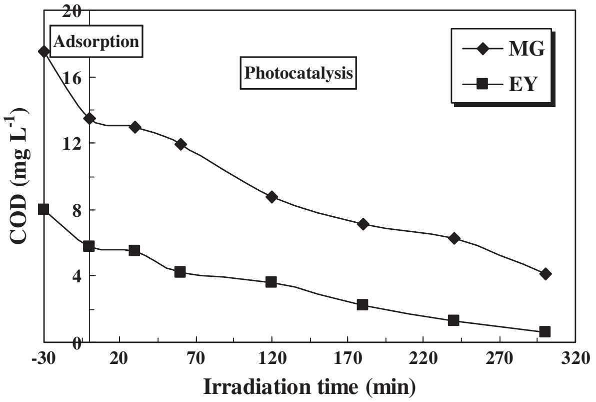

Fig. 3. Kinetics of COD disappearance of MG and EY by photocatalytic process with irradiation time: ([Dye] = 10 mg L^{-1}, [P25] = 1 g L^{-1}, $I = 2.5$ mW cm^{-2}, and at natural pH (≈6.3 ± 0.5)).

decolorization was achieved within 60 and 45 min, but the mineralization was only partly achieved 32 and 47% for MG and EY, respectively. This result would be explained by the fact that the dyes are not directly mineralized, but transformed in intermediate photoproducts. These generated photoproducts may submit other cycles of degradation to complete total mineralization. However, it is important to note that the rate of mineralization of an organic compound depends upon the area to volume ratio of reactor (*A*/*V* ratio) [25,26].

3.3. Comparison of different photocatalysts at different pH

According to the literature [15,27–30], the photocatalytic activity of suspended TiO_2 in solution strongly depends on the physical properties of TiO_2 (e.g. crystal structure, surface area, and particle size). The catalyst particles are generally amphoteric in nature and the photocatalytic process takes place on the surface of TiO_2. The pH of the solution has a strong influence on the surface properties of TiO_2 particle. The influence of various kinds of TiO_2 such as P25, PC50, PC100, PC105, and PC500 (1 g L^{-1}) on the adsorption and the photodegradation of MG and EY (10 mg L^{-1}) at natural (pH ≈ 6.3 ± 0.5), acidic (pH 3), and basic (pH 9) conditions has been studied, in order to compare their reactivity and investigate the effect of pH on the photocatalytic efficiency. The pH of the solutions was adjusted at the beginning and measured at the end of each experiment. For both dyes, pH of the reaction mixture at acidic medium remains nearly constant during the course of the experiments. However, at basic medium, pH decreases from 10 to (pH ≈ 6.3 ± 0.5) for all the catalysts, except for PC100 (from 10 to 4.8 for both dyes). The experimental results of the adsorbed quantities and the decolorization rate constants of MG and EY at natural, acidic, and basic mediums are plotted in Figs. 4 and 5, respectively.

The order of the catalyst's activities, at natural pH, for the degradation of MG is: P25 > PC50 > PC500 > PC105 > PC100, the same order was observed at acidic and basic conditions (Fig. 4); however, except the good correlation observed between the photocatalytic activity and the adsorbed quantity of MG at natural pH, no significant correlation was found at acidic and basic pH (inset in Fig. 4). In case of EY, the following activity order was obtained at natural pH: P25 > PC50 > PC100 > PC105 > PC500. Nevertheless, depending on the pH, this classification was modified. PC500 exhibited the highest adsorption and photoactivity at acidic medium, whereas, PC100 was more effective in adsorption and photocatalysis than the other TiO_2 samples at basic medium (Fig. 5 and inset shown in Fig. 5).

These results indicate that the surface and structural properties (crystalline phase, average crystalline size, and surface area) of the semiconductor play an important role in the photocatalytic activity of TiO_2 samples. In addition, the pH of the solution plays a major role in determining the efficiency of photocatalyst in the photocatalytic reaction.

The photocatalyst P25 has the highest degradation kinetics for both dyes at natural pH. The better photocatalytic activity of Degussa P25 for the degradation of large number of compounds has been reported earlier [28–30]. The main difference between Degussa P25 and Millennium photocatalysts is that P25 consists a mixture of 80% anatase and 20% rutile, whereas Millennium photocatalysts are made of a pure anatase phase. Pure anatase phase is the most active crystalline phase in comparison with pure rutile [31]. P25 is made of three phases, a pure anatase phase, a pure rutile phase, and anatase nuclei inside a rutile layer phase [32]. The particles of this third phase would be responsible for the high efficiency of P25. The conduction band of rutile is considered to be a lower level than that of anatase. As shown in Fig. 6, the coupling of two phases allows the vectorial displacement of electrons from anatase to the rutile particle and retards the recombination of electron–hole pairs in anatase. Consequently, electrons and holes are available more for the reduction and oxidation reactions.

Moreover, the photocatalyst PC50 (100% anatase) was shown to be the second most efficient catalyst after P25 for the degradation of both dyes. It is interesting to remark that the two catalysts having the highest degradation kinetics with both dyes are those with the largest particles' size: P25 (20 nm) and PC50

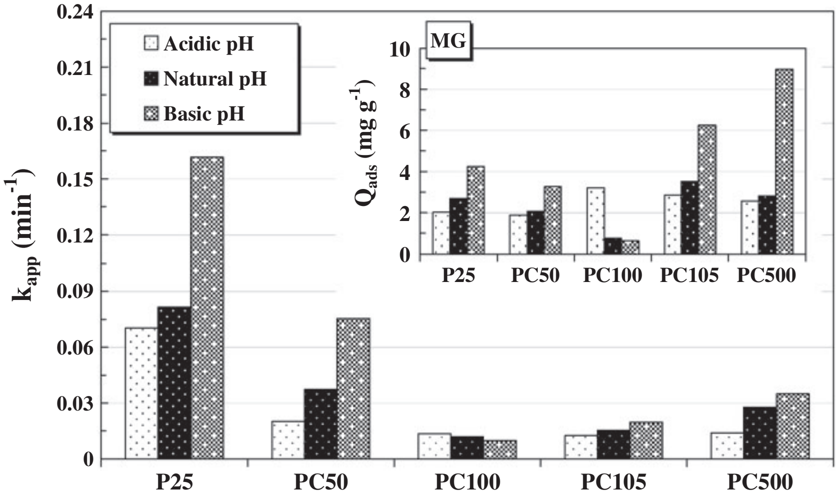

Fig. 4. Effect of pH on the photocatalytic degradation of MG by different types of TiO_2 catalysts. In the inset: effect of pH on the amounts of MG adsorbed on TiO_2: ([MG] = 10 mg L^{-1}, [catalyst] = 1 g L^{-1}, and I = 2.5 mW cm^{-2}).

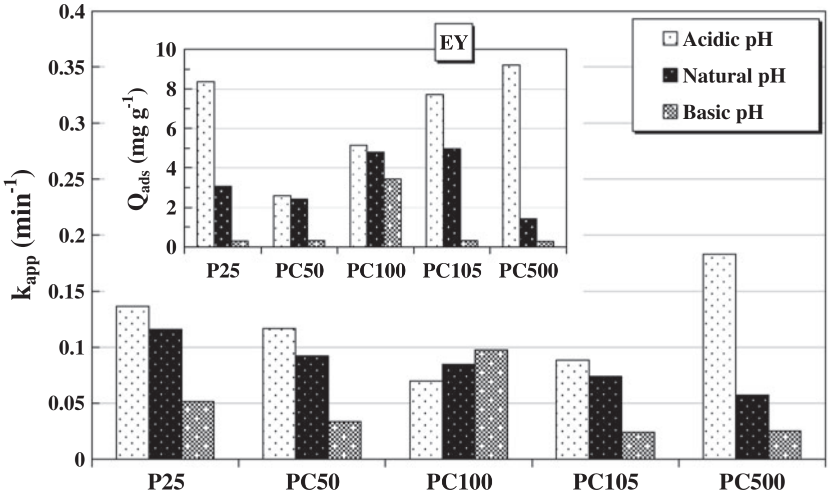

Fig. 5. Effect of pH on the photocatalytic degradation of EY by different types of TiO_2 catalysts. In the inset: effect of pH on the amounts of EY adsorbed on TiO_2: ([EY] = 10 mg L^{-1}, [catalyst] = 1 g L^{-1}, and I = 2.5 mW cm^{-2}).

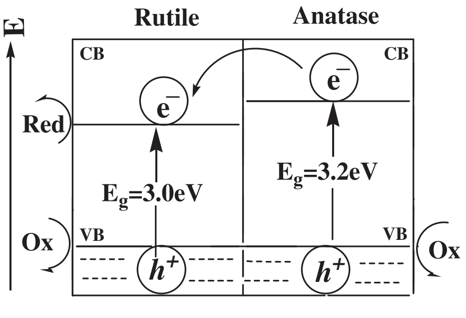

Fig. 6. Energy diagram for the heterogeneous anatase/rutile TiO_2.

(19 nm), and the smallest surface area: P25 (55 m^2 g^{-1}) and PC50 (45 ± 5 m^2 g^{-1}) of all the TiO_2 investigated. Indeed, other studies reported that TiO_2 with larger particles and lower surface area performed better in the degradation of a number of organic compounds than TiO_2 with smaller particles and larger surface area [33,34]. This behavior was attributed to a lower scattering in the UV range of photocatalysts having larger particles. This observation is confirmed by the low activity of two catalysts with highest specific surface area: PC500 (345 m^2 g^{-1}) to degrade both dyes and PC100 (80 m^2 g^{-1}) to degrade MG, showing that a large surface area is not always necessarily an

advantage to degrade a pollutant onto TiO_2, as previously reported. Nevertheless, PC100 has a good photocatalytic efficiency to degrade EY, this could be related, as described above, to the decrease of pH in the presence of PC100 at the end of experiment (4.9), which leads to electrostatic attraction between the negatively charged molecule of EY and the positive surface of PC100.

3.3.1. At different pH

From Fig. 5, it can be seen that the adsorbed quantity and the decolorization rate constant of the anionic dye EY increase with decrease in the pH exhibiting a maximum rate of degradation at acidic medium. An opposite effect of pH is observed for the cationic dye MG, where the dye adsorption and removal were better in alkaline pH than in acidic and natural pH (Fig. 4). The same trend was observed for all the TiO_2 catalysts except for PC100. The strong influence of pH on the degradation of both dyes depends on the specific nature of TiO_2 surface and the intrinsic behavior of TiO_2 [35] and also the nature of the dye (anionic or cationic). The point of zero charge (pzc) of TiO_2 in water is at pH ≈ 6.0 ± 0.8 [11,36]. Thus, at more acidic pH, the particle surface is positively charged ($TiOH_2^+$), while at pH > pzc, it is negatively charged (TiO^-). The functional group present on the dye can be protonated and deprotonated depending on the pH of the reaction mixture. The better degradation rate in acidic or basic pH may also be attributed on the basis of the fact that the structural orientation of the molecule is favored for the attack of the reactive species under that condition. Since MG is a cationic dye (positively charged ($=N^+(CH_3)_2$)), it is conceivable that at high pH values, its adsorption is favored on a negatively charged surface through electrostatic force of attraction. By contrast, EY is an anionic dye and its adsorption is inhibited at high pH values because of the columbic repulsion between the dye with negatively charged (COO^-) function and the surface of catalyst (TiO^-). At lower pH, the surface of photocatalyst gets positively charged ($TiOH_2^+$), which enhances the adsorption of the negatively charged EY ions and decreases the adsorption of the cationic dye MG (Fig. 7).

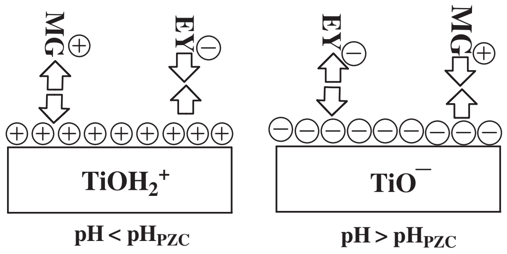

Fig. 7. Ionization of titania surface as a function of the pH.

3.3.2. Proton sources of acidic pH

The acid used to adjust pH dissociates in water into protons (H^+) and ions, these ions can interfere with the dye degradation efficiency. To investigate the effect of proton sources of pH on the adsorption and decolorization of both dyes by different types of TiO_2 (P25, PC50, PC100, PC105, and PC500), pH was adjusted at pH 3 using three different acids: sulfuric acid (H_2SO_4) ($pK_{a1} \approx -3$), hydrochloric acid (HCl) ($pK_a = -6.3$), and perchloric acid ($HClO_4$) ($pK_a \approx -8$), (Figs. 8 and 9). The results clearly have shown that the rate constant of degradation of both dyes depends on the nature of the acid used and are directly related to the counter ion of each acid. For all the catalysts tested, the decolorization rate varies with varying the anions in the order: $SO_4^{2-} > Cl^- > ClO_4^-$ for both MG and EY dyes. These results are correlated with the adsorbed quantities for the anionic dye (EY) (inset in Fig. 9). However, no significant correlation was observed between the adsorption and the degradation rate for cationic dye (MG) (inset in Fig. 8).

It is interesting to remark that the degradation rates of both dyes are inversely correlated with the order of the dissociation degree of the three acids ($HCLO_4 > HCl > H_2SO_4$). A high dissociation degree results in an enhancement in the ions' concentrations in solution, which is capable of inhibiting the photocatalytic degradation of dyes due to the reduction of light absorption by the photocatalyst induced by ions. The enhancement of the reaction rate in the presence of H_2SO_4 for both dyes can be also explained by the inhibition of electron–hole recombination and production of other oxidizing species sulfate radical anions. The sulfate radical anion ($SO_4^{\bullet-}$) is a very strong oxidant ($E^\circ = 2.6$ eV). This radical anion can also participate in the degradation process in the following way [37]:

$$H_2SO_4 \rightarrow SO_4^{2-} + 2H^+ \tag{7}$$

$$SO_4^{2-} + h_{VB}^+ \rightarrow SO_4^{\bullet-} \tag{8}$$

$$SO_4^{\bullet-} + \text{Dye} \rightarrow SO_4^{2-} + \text{Dye intermediate} \tag{9}$$

In contrast, if the proton source was replaced by other acids (HCl or $HClO_4$), retardation of the reaction rates of both dyes was observed (Figs. 8 and 9). This can be

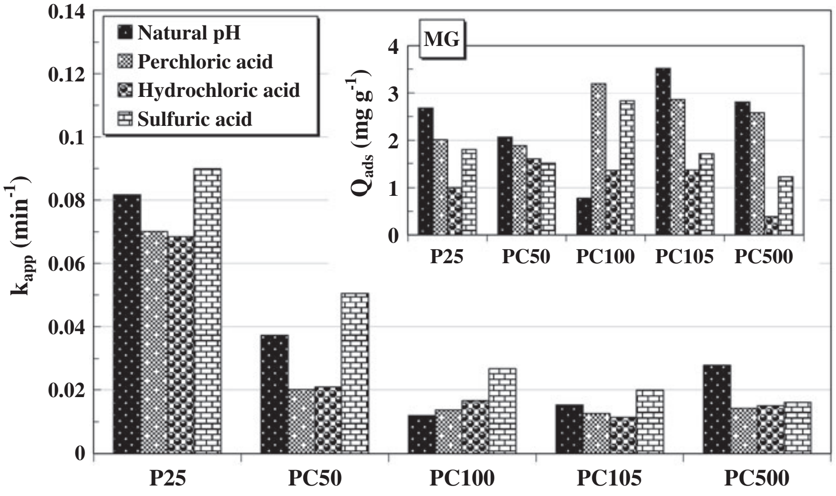

Fig. 8. Effect of proton sources of pH on the decolorization of MG by different catalysts. In the inset: effect of proton sources of pH on the amounts of MG adsorbed on TiO_2: ([MG] = 10 mg L^{-1}, [catalyst] = 1 g L^{-1}, and I = 2.5 mW cm^{-2}).

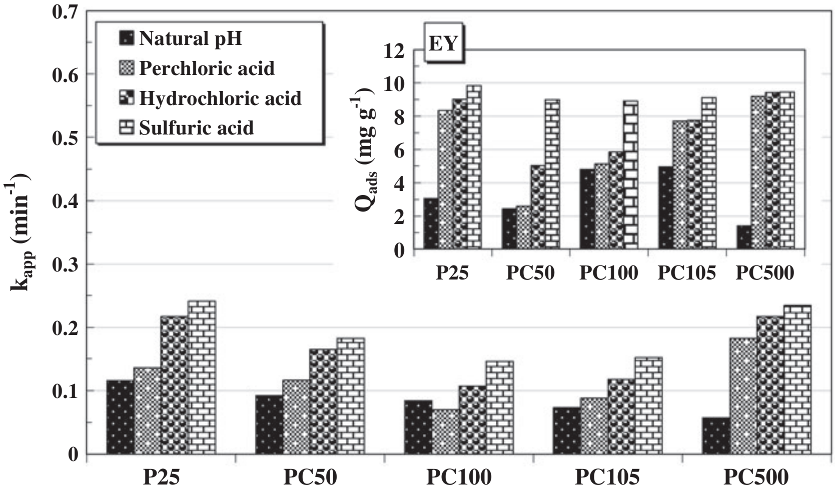

Fig. 9. Effect of proton sources of pH on the decolorization of EY by different catalysts. In the inset: effect of proton sources of pH on the amounts of EY adsorbed on TiO_2: ([EY] = 10 mg L^{-1}, [catalyst]= 1 g L^{-1}, and I = 2.5 mW cm^{-2}).

explained on the basis that the presence of these ions scavenges the holes and hydroxyl radicals according to the following reactions (Eqs. (10)–(13)), thus causing a decrease in decolorization [38].

$$Cl^- + h^+_{VB} \rightarrow Cl^\cdot \quad (10)$$

$$Cl^- + {}^\cdot OH \rightarrow OH^- + Cl^\cdot \quad (11)$$

$$ClO_4^- + h^+_{VB} \rightarrow ClO_4^\cdot \quad (12)$$

$$ClO_4^- + {}^\cdot OH \rightarrow ClO_4^\cdot + OH^- \quad (13)$$

3.4. Effect of H_2O_2 addition

The effect of H_2O_2 addition on the photocatalytic degradation of both dyes by TiO_2-P25 (1 g L^{-1}) was studied by varying the concentration of H_2O_2 ranging from 10^{-4} to 10^{-1} mol L^{-1} and fixing the dye concentration at 10 mg L^{-1} at natural pH (pH ≈ 6.3 ± 0.5). Fig. 10 shows the changes of the rate constant of the photocatalytic decolorization and the adsorbed amount of dyes on the photocatalyst (inset in Fig. 10) as a function of H_2O_2 concentrations.

The decolorization rate of MG and EY increases with an increase in the H_2O_2 concentration from 10^{-4} to 10^{-3} mol L^{-1} and a maximum value appears at

10^{-3} mol L^{-1} for both dyes; the shape of the curves of adsorbed quantity of both dyes is similar to that of their degradation rates, showing a reasonable correlation between the amount of dyes adsorbed and their degradation efficiency. The enhancement of decolorization by addition of H_2O_2 is due to an increase in the hydroxyl radical ${}^\bullet OH$ concentration, since it inhibits the e^-–h^+ recombination, according to the following equations [39]:

$$H_2O_2 + e^-_{CB} \rightarrow OH^- + {}^\bullet OH \tag{14}$$

$$H_2O_2 + O_2^{\bullet -} \rightarrow {}^\bullet OH + OH^- + O_2 \tag{15}$$

However, a further increase in the H_2O_2 concentration from 10^{-3} to 10^{-1} mol L^{-1} decreases the decolorization rate of EY from 0.175 to 0.032 min^{-1} and the decolorization rate constant of MG reaches a plateau. The excess of H_2O_2 consumes hydroxyl radicals and it performs like hydroxyl radical scavengers, according to the following equations [40,41]:

$$H_2O_2 + {}^\bullet OH \rightarrow HO_2^\bullet + H_2O \tag{16}$$

$$HO_2^\bullet + {}^\bullet OH \rightarrow H_2O + O_2 \tag{17}$$

3.4.1. At different pH

The effect of initial pH on MG and EY (10 mg L^{-1}) photodegradation and adsorption with the addition of an optimal dosage of H_2O_2 (10^{-3} mol L^{-1}) was then studied at natural (pH ≈ 6.3 ± 0.5), acidic (pH 3), and basic (pH 9) conditions; the results are illustrated in Figs. 11 and 12 for MG and EY, respectively. The variation of rate constants with initial pH was similar to photocatalysis experiments without adding H_2O_2. The adsorbed quantity and the disappearance of the cationic dye (MG) increase at basic pH. While, in the case of the anionic dye (EY), the adsorbed quantity and the degradation rate were relatively high at acidic pH, and an optimum degradation was found at natural medium, similar results have been reported by Chu and Wong on the Dicamba degradation by the H_2O_2-assisted photocatalysis in TiO_2 suspensions, in a range of pH from 1 to 11; the reaction rates of Dicamba gradually increased with increments in the initial pH level, and an optimal pH was found as 6, and the further elevation of solution pH retarded the rates [42]. The results obtained in this study are related to the ionization state of the catalyst surface and the charge of the dye studied. Another important point to underline is that the enhancement of the degradation efficiency of both dyes by the UV/TiO_2/H_2O_2 process compared to the UV/TiO_2 process was more pronounced at natural and acidic mediums than that at alkaline medium. In an alkaline medium, H_2O_2 becomes unstable and rapidly decays into water and oxygen, even in the presence of UV light [43]. This assumption can be justified by the rate constant obtained at alkaline pH in the UV/TiO_2/H_2O_2 process of both dyes which was about the same as that in the photocatalysis experiment without the addition of H_2O_2.

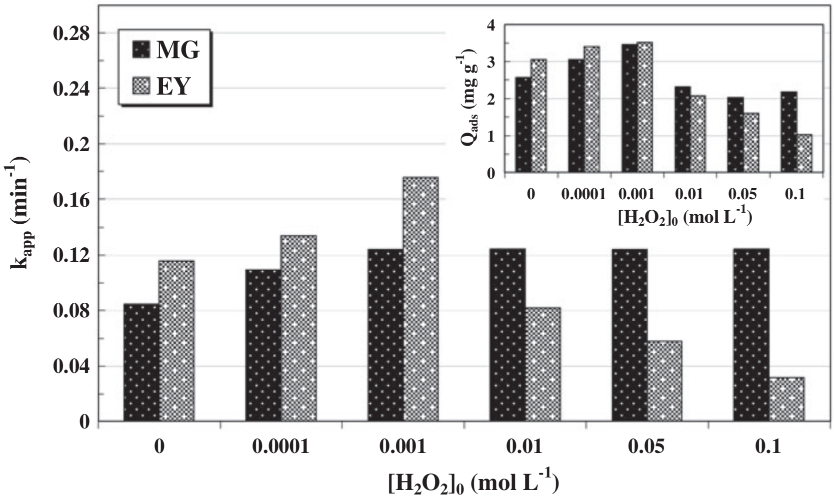

Fig. 10. Effect of H_2O_2 concentration on the photocatalytic degradation of MG and EY. In the inset: effect of H_2O_2 concentration on the amounts of MG and EY adsorbed on TiO_2: ([Dye] = 10 mg L^{-1}, [P25] = 1 g L^{-1}, I = 2.5 mW cm^{-2}, and at natural pH (6.3 ± 0.5)).

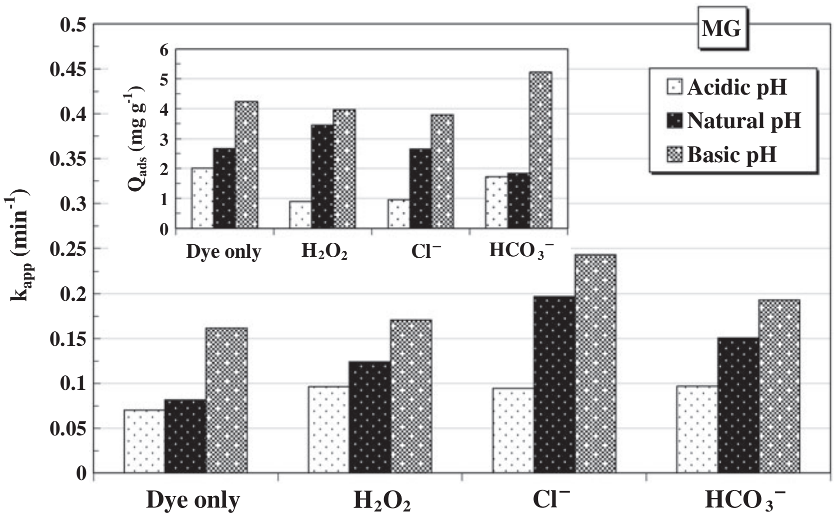

Fig. 11. Effect of pH on the photocatalytic activity of MG in the presence of H_2O_2, Cl^- and HCO_3^-. In the inset: effect of pH on the amounts of MG adsorbed on TiO_2: ([MG] = 10 mg L^{-1}, [P25] = 1 g L^{-1}, and I = 2.5 mW cm^{-2}).

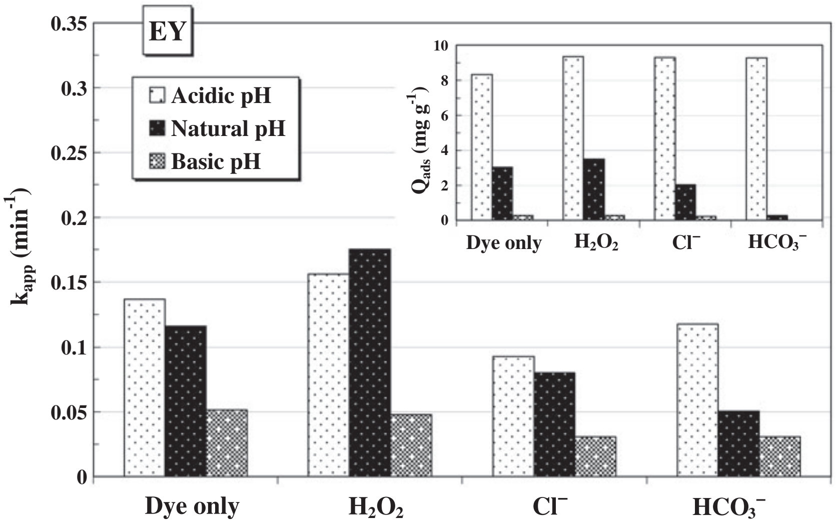

Fig. 12. Effect of pH on the photocatalytic activity of EY in the presence of H_2O_2, Cl^- and HCO_3^-. In the inset: effect of pH on the amounts of EY adsorbed on TiO_2: ([EY] = 10 mg L^{-1}, [P25] = 1 g L^{-1}, and I = 2.5 mW cm^{-2}).

3.5. Effect of inorganic anions addition

Wastewaters and natural water systems contain a variety of inorganic species that interfere with oxidation reactions of ·OH with the target contaminants. Of these, the inorganic anions such as chloride and bicarbonate are very common. Bicarbonate ions are frequently found in natural waters, whereas chloride exists in high concentrations in landfill leachate, tannery, and dye-manufacturing wastewaters [44]. To investigate the effect of these salts on the adsorption and the photocatalytic reaction, NaCl and $NaHCO_3$ were added at different concentrations from 10^{-4} to 10^{-1} mol L^{-1} in the solution of MG and EY, results are shown in Figs. 13 and 14. Furthermore, the effect of NaCl and $NaHCO_3$, at a fixed concentration (10^{-3} mol L^{-1}), was also investigated at different initial pH: natural (pH ≈ 6.3 ± 0.5), acidic (pH 3), and basic (pH 9) of MG and EY solutions. The results are shown in Figs. 11 and 12.

3.5.1. Effect of Cl^-

The effect of Cl^- ions on the photocatalytic degradation of organic pollutants has been discussed in many papers [45,46]. In many of them, an inhibiting effect was reported due to two possible effects. The first one is the competitive adsorption between the pollutant molecules and ions for the surface active sites of TiO_2 which leads to reduced photocatalytic efficiency of the process. The second one is the potential scavenging function of anions, they can react with photogenerated holes and consequently reduce the number of oxidizing species for the degradation of pollutant molecules. However, the inhibiting or accelerating effect of Cl^- ions on the degradation efficiency depends on several factors such as chloride concentrations, the chemical structure of pollutant, and pH of solution.

In the present study, the increase in Cl^- ion concentrations decreases significantly the adsorbed quantity and the decolorization rate constant of EY. In contrast, in the case of MG, the presence of these ions enhances decolorization of the dye and maximum degradation is observed at a low concentration of the salt (10^{-4} mol L^{-1}) (Fig. 13). A good correlation was observed between the adsorption of both dyes on TiO_2 surface and the rate of photodegradation in the presence of Cl^- species (inset in Fig. 13).

Inhibition effect of Cl^- on the photocatalytic activity of EY is due to the reaction of hydroxyl radicals and positive holes with chloride anions (Eqs. (10) and (11)) that behaved as $^{\cdot}OH$ and h^+ scavengers resulting in a prolonged color removal, and the competitive adsorption between the dye and the anions can be envisaged to explain the inhibition of EY adsorption [47].

The inhibiting effect of Cl^- only in case of EY but not in case of MG may be because it is an anionic dye, whereas MG is a cationic dye; degradation due to direct attack of holes is not possible in the case of cationic dyes. In addition, the electrical charges on the photocatalyst surface are neutralized at the reaction pH (6.8) of the MG solution (pH_{pzc} = 6.8). Thus, addition of Cl^- has no influence on the adsorption of MG to TiO_2 and there is no competition with dye molecules for surface active sites. Most probable hypothesis may explain the apparent increase of the degradation of MG is certainly that the chloride radicals $Cl^{\cdot}$ that are formed (Eqs. (10) and (11)) can react with the dye. However, they have a lower oxidation potential than $^{\cdot}OH$ [48,49].

3.5.1.1. At different pH. Considering Figs. 11 and 12, it is clear that the effect of chloride ions on the adsorption and degradations of both dyes is pH dependent. Furthermore, both the adsorption and the degradation of EY were inhibited in the presence of Cl^- at different pH mediums studied compared to the dye only. In addition, this inhibition effect was more remarked at acidic pH than at natural and basic pH. However, in the case of MG, an increase in both adsorption and degradation was observed at different pH mediums tested compared to dye only, and this acceleration was less pronounced at acidic pH. These results are directly correlated with the charge of the molecule studied and the ionization state of the catalyst surface.

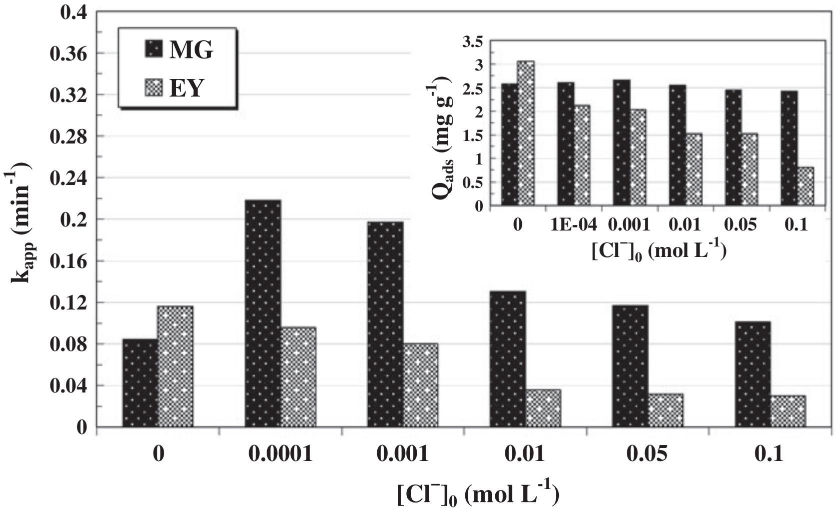

Fig. 13. Effect of Cl^- on photocatalytic decolorization of MG and EY in presence of TiO_2. In the inset: effect of Cl^- on MG and EY adsorption on TiO_2: ([Dye] = 10 mg L^{-1}, [P25] = 1 g L^{-1}, I = 2.5 mW cm^{-2}, and at natural pH (6.3 ± 0.5)).

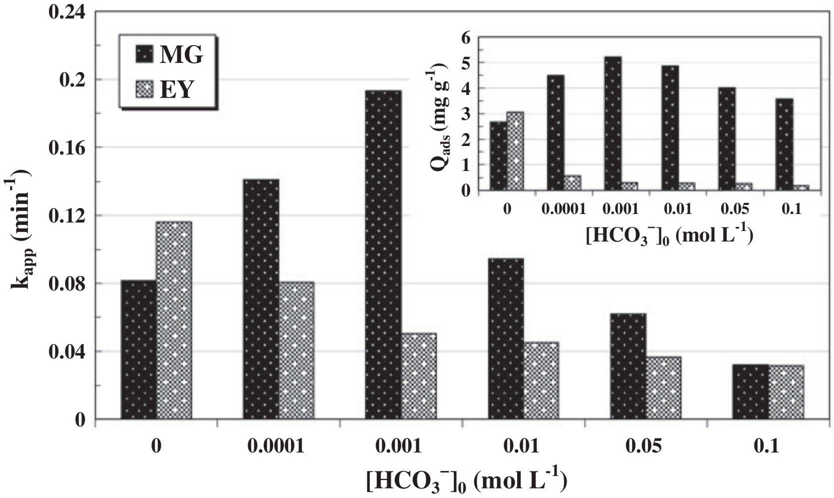

Fig. 14. Effect of HCO_3^- on photocatalytic decolorization of MG and EY in presence of TiO_2. In the inset: effect of HCO_3^- on MG and EY adsorption on TiO_2: ([Dye] = 10 mg L^{-1}, [P25] = 1 g L^{-1}, I = 2.5 mW cm^{-2}, and pH ≈ 8.3).

3.5.2. *Effect of HCO_3^-*

In general, the effect of bicarbonate ions' addition on the dye photocatalytic degradation is difficult to explain, since it had multiple roles because it acts both as a scavenger of hydroxyl radical and a source of carbonate radical. As shown in Fig. 14, the degradation of EY decreases with an increase in the bicarbonate ion concentrations, and a linear correlation was observed between the adsorbed quantity and the rate constant of EY degradation (inset in Fig. 14). Contrary to EY, the addition of bicarbonate ions increases the rate of MG degradation and an optimum value was observed at a low concentration of HCO_3^- (10^{-3} mol L^{-1}), and it takes relatively very high concentrations of HCO_3^- (5×10^{-2} mol L^{-1}) to reduce slightly the decolorization rate; these results are correlated with the adsorbed quantity of MG (inset in Fig. 14).

The inhibition of the degradation efficiency of the anionic dye EY is due to hydroxyl radical-scavenging property of bicarbonate ions as shown in the following equation:

$$HCO_3^- + {}^{\bullet}OH \rightarrow H_2O + CO_3^{\bullet -} \quad k = 8.5 \times 10^6\ M^{-1}\ S^{-1} \tag{18}$$

Thus, the primary oxidant hydroxyl radical decreases gradually with the increase in the bicarbonate ions and consequently, there is a significant decrease in the photocatalytic degradation [47].

However, in the case of cationic dye MG, the addition of HCO_3^- has an alkaline effect on the solution of MG; addition of $NaHCO_3$ maintains the pH of solution around 8.3 (HCO_3^- is the predominant species as pK_a (HCO_3^-/CO_3^{2-}) = 10.2). Thus, since MG is a cationic dye, it is positively charged in alkaline medium, whereas, the surface of TiO_2 will be negatively charged which leads to an electrostatic attraction between MG molecules and TiO_2 surface and adsorption could occur [50], and consequently, the efficiency of the photocatalytic process increases.

3.5.2.1. At different pH. Figs. 11 and 12 show that the photocatalytic degradation of both dyes in the presence of HCO_3^- ions is mainly dependent on the solution pH. In the case of cationic dye, the MG degradation rate at alkaline medium is larger than that at natural and acidic mediums (Fig. 11). Since the adsorption of the dye is high at alkaline pH (inset in Fig. 11), the degradation is also efficient at these conditions. This reveals that the adsorption of MG on the surface of TiO_2 plays a vital role in the degradation mechanism. The higher efficiency of degradation in alkaline medium may be attributed also to the pH-dependent potential to generate $CO_3^{\bullet -}$ radicals because a basic medium has a high content of both HCO_3^- and CO_3^{2-}, which can absorb UV radiation and form $CO_3^{\bullet -}$ by the reactions (19) and (20) [51]. However, at natural pH (pH 6.3 after addition of bicarbonate ions), only HCO_3^- ions are present in the solution, the lesser degradation of MG is due to the low formation of bicarbonate radical ($HCO_3^{\bullet}$).

$$ {}^{\bullet}OH + HCO_3^- \rightarrow HCO_3^{\bullet} + OH^- \tag{19}$$

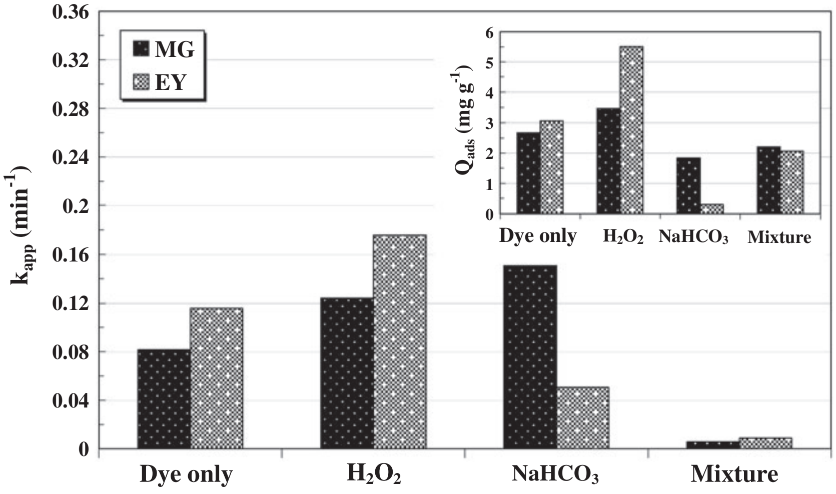

Fig. 15. Effect of simultaneous presence of H_2O_2 and $NaHCO_3$ on the degradation efficiency of MG and EY in the presence of TiO_2. In the inset: effect of simultaneous presence of H_2O_2 and $NaHCO_3$ on MG and EY adsorption on TiO_2: ([Dye] = 10 mg L^{-1}, [H_2O_2] = [$NaHCO_3$] = 10^{-3} mol L^{-1}, [P25] = 1 g L^{-1}, I = 2.5 mW cm^{-2}, and at natural pH (6.3 ± 0.5)).

$$\mathrm{HCO_3^{\bullet}} \overset{\mathrm{H_2O}}{\Leftrightarrow} \mathrm{H_3O^+ + CO_3^{\bullet -}} \qquad (20)$$

In contrast, most of the added carbonate ions are converted to CO_2 at acidic pH and a fraction of this CO_2 escapes into the atmosphere, reducing the possibility of generating $CO_3^{\bullet -}$ radicals in acidic medium (Eq. (21)). This can explain the decrease in the degradation of MG in the presence of bicarbonate ions at acidic medium.

$$\mathrm{HCO_3^- + H^+ \rightarrow H_2O + CO_2} \qquad (21)$$

In the case of the anionic dye, it can be seen that the adsorption and the rate of removal of EY decrease in the presence of bicarbonate ions in the following order: acidic > natural > alkaline (Fig. 12 and inset in Fig. 12). The observed decrease in the photodegradation rate of EY with the increase in the pH could be explained by the ability of bicarbonate ions to scavenge both holes and $^{\bullet}OH$ as functions of pH solution. The inhibition effect of bicarbonate ions was negligible under acidic pH (HCO_3^- dissociates) than other mediums.

3.6. Effect of simultaneous presence of HCO_3^- and H_2O_2

To investigate the simultaneous effect of inorganic anions, such as bicarbonate, on the scavenging of hydroxyl radicals in the UV/TiO_2/H_2O_2 process, the degradation of MG and EY dyes (10 mg L^{-1}) was studied in the presence of HCO_3^- (10^{-3} mol L^{-1}) and H_2O_2 (10^{-3} mol L^{-1}). As can be seen in Fig. 15, the rate of degradation of both dyes has been significantly inhibited in the presence of the mixture of H_2O_2 and HCO_3^-. The inset of Fig. 15 shows that the adsorbed quantity of both dyes in the presence of mixture is also inhibited compared with that obtained in the presence of only dye. The inhibition of both dyes' degradation in the presence of mixture can be explained by the interaction between H_2O_2 and $NaHCO_3$ during the photocatalytic reaction. Bicarbonate ions are well known as hydroxyl radical scavengers; therefore, their excess concentration can affect the destruction of the target contaminant and ultimately reduce the effectiveness of the UV/TiO_2/H_2O_2 process. The reaction of $^{\bullet}OH$ with HCO_3^- generates carbonate radicals $CO_3^{\bullet -}$ (Eqs. (19) and (20)), which are equally reactive with reducing species in solution. On the other hand, carbonate radicals may react with H_2O_2 to produce other radical species such as peroxy radicals ($HO_2^{\bullet}$) (Eq. (22)), which may contribute to dye degradation by oxidative action, however, at a much slower rate than the reaction of $^{\bullet}OH$.

$$\mathrm{H_2O_2 + CO_3^{\bullet -} \rightarrow HCO_3^- + HO_2^{\bullet}} \quad k = 4.3 \times 10^5\ \mathrm{M^{-1}\ S^{-1}} \qquad (22)$$

The presence of HCO_3^- in solution also interferes with H_2O_2 for UV light, decreasing the fraction it normally absorbs. This in turn slows down the rate of hydroxyl radical generation [52].

4. Conclusion

Both Malachite green oxalate (MG) and Eosin yellow (EY) dyes are easily degraded by TiO_2 photocatalysis in aqueous dispersion under UV-A irradiation. The fast decolorization and mineralization of the anionic dye EY compared to the cationic dye MG at natural pH are indications that the type of dye, its ionic character, and its molecular formula may be determining factors influencing the degradation rate. The mixed crystalline structure, TiO_2 P25, showed a higher photoactivity to degrade both dyes than pure anatase TiO_2. In addition, TiO_2 with larger particles and lower surface area (P25 and PC50) performed better in the degradation of both dyes in comparison with smaller particles and larger surface area (PC500 and PC100). With almost all the catalysts tested, the decolorization rate of the anionic dye EY was significantly increased at acidic conditions, whereas an enhancement of the decolorization was found at alkaline conditions for the cationic dye MG; this opposite effect is directly correlated with the ionization state of the catalyst surface and the charge of the molecule studied. The decolorization rate of both dyes varies with varying the acid used to adjust the pH in the order: $H_2SO_4 > HCl \geq HClO_4$. An enhancement of the degradation rate constants of both dyes was observed for the lower concentrations of H_2O_2 in the presence of P25. Inorganic anions inhibit the adsorption and the photocatalytic decolorization of EY and contrasting for MG. The strong inhibiting or accelerating effect of these ions depends in a complicated way of pH, salt type, and salt concentration. The rate of degradation of both dyes has been significantly inhibited in the presence of mixture of H_2O_2 and HCO_3^-; this is related to their interaction during the photocatalytic reaction. In all the experiments, the photocatalytic degradation of both dyes was generally found to be correlated with adsorption in the dark.

Acknowledgment

This work was financially supported by the Ministry of Higher Education and Scientific Research of Algeria.

References

[1] J.J. Porter, A Study of the Photo-Degradation of Commercial Dyes, Environmental Protection Agency Report-R2-73-058, Washington, DC, 1973.

[2] S. Dai, W. Song, T. Li, Y. Zhuang, Study on Azo Dyes structure biodegradability relationships, Adv. Environ. Sci. 4 (1996) 1–9.

[3] J.G. Montano, X. Domènech, J.A. García-Hortal, F. Torrades, J. Peral, The testing of several biological and chemical coupled treatments for Cibacron Red FN-R azo dye removal, J. Hazard. Mater. 154 (2008) 484–490.

[4] N. Daneshvar, D. Salari, A.R. Khataee, Photocatalytic degradation of azo dye acid red 14 in water: Investigation of the effect of operational parameters, J. Photochem. Photobiol. A. 157 (2003) 111–116.

[5] E. Vulliet, J.M. Chovelon, C. Guillard, J.M. Herrmann, Factors influencing the photocatalytic degradation of sulfonylurea herbicides by TiO_2 aqueous suspension, J. Photochem. Photobiol. A. 159 (2003) 71–79.

[6] T.P. Dhanya, S. Sugunan, Preparation, characterization and photocatalytic activity of N doped TiO_2, IOSR J. Appl. Chem. IOSR-JAC. 4 (2013) 2278–5736.

[7] C.G. Silva, W. Wang, J.L. Faria, Photocatalytic and photochemical degradation of mono-, di- and tri-azo dyes in aqueous solution under UV irradiation, J. Photochem. Photobiol. A: Chem. 181 (2006) 314–324.

[8] W. Baran, A. Makowski, W. Wardas, The effect of UV radiation absorption of cationic and anionic dye solutions on their photocatalytic degradation in the presence TiO_2, Dyes Pigm. 76 (2008) 226–230.

[9] M.A. Barakat, Adsorption and photodegradation of Procion yellow H-EXL dye in textile wastewater over TiO_2 suspension, J. Hydro-Environ. Res. 5 (2011) 137–142.

[10] A. Mills, S. LeHunte, An overview of semiconductor photocatalysis, J. Photochem. Photobiol. A. 108 (1997) 1–35.

[11] A. Rachel, M. Sarakha, M. Subrahmanyam, P. Boule, Comparison of several titanium dioxides for the photocatalytic degradation of benzenesulfonic acids, Appl. Catal. B: Environ. 37 (2002) 293–300.

[12] A. Amine-Khodja, A. Boulkamh, C. Richard, Phototransformation of metobromuron in the presence of TiO_2, Appl. Catal. B: Environ. 59 (2005) 147–154.

[13] I. Liu, L.A. Lawton, D.W. Bahnemann, L. Liu, B. Proft, P.K.J. Robertson, The photocatalytic decomposition of using selected titanium dioxide materials, in comparing to the four commercial, Chemosphere. 76 (2009) 549–553.

[14] N. Mezioud, N. Bouziane, M.A. Malouki, A. Zertal, Methabenzthiazuron degradation with illuminated TiO_2 aqueous suspensions. Kinetic and reactional pathway investigations, J. Photochem. Photobiol. A. 288 (2014) 13–22.

[15] N. Bouanimba, R. Zouaghi, N. Laid, T. Sehili, Factors influencing the photocatalytic decolorization of Bromophenol blue in aqueous solution with different types of TiO_2 as photocatalysts, Desalination. 275 (2011) 224–230.

[16] M.R. Hoffmann, S.T. Martin, W. Choi, D.W. Bahnemann, Environmental applications of semiconductor photocatalysis, Chem. Rev. 95 (1995) 69–96.

[17] S.J. Culp, P.W. Mellick, R.W. Trotter, K.J. Greenlees, R.L. Kodell, F.A. Beland, Carcinogenicity of malachite green chloride and leucomalachite green in B6C3F1 mice and F344 rats, Food Chem. Toxicol. 44 (2006) 1204–1212.

[18] H. Zheng, Y. Pan, X. Xiang, Oxidation of acidic dye Eosin Y by the solar photo-Fenton processes, J. Hazard. Mater. 141 (2007) 457–464.

[19] S.J. Culp, A. Frederick, Malachite Green: A toxicological review, Int. J. Toxicol. 15 (1996) 3219–3238.

[20] I. Poulios, E. Micropoulou, R. Panou, E. Kostopoulou, Photooxidation of eosin Y in the presence of semiconducting oxides, Appl. Catal. B: Environ. 41 (2003) 345–355.

[21] R.J. Tayade, P.K. Surolia, R.G. Kulkarni, R.V. Jasra, Photocatalytic degradation of dyes and organic contaminants in water using nanocrystalline anatase and rutile TiO_2, Sci. Technol. Adv. Mater. 8 (2007) 455.

[22] O. Thomas, N. Mazas, La mesure de la demande chimique en oxygène dans les milieux faiblement pollués (Measuring chemical demand oxygen in weakly polluted mediums), Analusis 14 (1986) 300–302.

[23] A.R. Khataee, M.B. Kasiri, Photocatalytic degradation of organic dyes in the presence of nanostructured titanium dioxide: Influence of the chemical structure of dyes, J. Mol. Catal. A: Chem. 328 (2010) 8–26.

[24] H.F. Moafi, A.F. Shojaie, M.A. Zanjanchi, The comparison of photocatalytic activity of synthesized TiO_2 and ZrO_2 nanosize onto wool fibers, Appl. Surf. Sci. 256 (2010) 4310–4316.

[25] S.K. Sharma, H. Bhunia, P.K. Bajpai, Photocatalytic decolorization kinetics and mineralization of Reactive Black 5 aqueous solution by UV/TiO_2 nanoparticles, Clean—Soil, Air, Water 40 (2012) 1290–1296.

[26] S.K. Sharma, H. Bhunia, P.K. Bajpai, TiO_2-assisted photocatalytic degradation of Diazo Dye Reactive Red 120: Decolorization kinetics and mineralization investigations, J. Adv. Oxid. Technol. 16 (2013) 306–313.

[27] T.Y. Wei, C.C. Wan, Heterogeneous photocatalytic oxidation of phenol with titanium dioxide powders, Ind. Eng. Chem. Res. 30 (1991) 1293–1300.

[28] A. Khan, M.M. Haque, N.A. Mir, M. Muneer, C. Boxall, Heterogeneous photocatalysed degradation of an insecticide derivative acetamiprid in aqueous suspensions of semiconductor, Desalination 261 (2010) 169–174.

[29] C. Guillard, N. Perol, J.M. Hermann, Photocatalytic degradation of imazapyr in water: Comparison of activities of different supported and unsupported TiO_2 based catalysts, Catal. Today 101 (2005) 211–218.

[30] A. Niyaz. Mir, A. Khan, M. Muneer, S. Vijayalakhsmi, Photocatalytic degradation of a widely used insecticide Thiamethoxam in aqueous suspension of TiO_2: Adsorption, kinetics, product analysis and toxicity assessment, Sci. Total Environ. 458–460 (2013) 388–398.

[31] K. Tanaka, T. Hisanaga, P. Rivera, D.F. Ollis, H. Al-Ekabi, Photocatalytic Purification and Treatment of Water and Air, Elsevier, Amsterdam, 1993, pp. 169–178.

[32] R.I. Bickley, T. Gonzalez-Carreno, J.S. Lees, L. Palmisano, R.J.D. Tilley, A structural investigation of titanium dioxide photocatalysts, J. Solid State Chem. 92 (1991) 178.

[33] D. Vione, C. Minero, V. Maurino, M.E. Carlotti, T. Picatonotto, E. Pelizzetti, Degradation of phenol and benzoic acid in the presence of a TiO_2-based heterogeneous photocatalyst, Appl. Catal. B: Environ. 58 (2005) 79–88.

[34] C. Minero, D. Vione, A quantitative evalution of the photocatalytic performance of TiO_2 slurries, Appl. Catal. B: Environ. 67 (2006) 257–269.

[35] K. Tanaka, K. Padermpole, T. Hisanaga, Photocatalytic degradation of commercial azo dyes, Water Res. 34 (2000) 327–333.

[36] D.E. Kritikos, N.P. Xekoukoulotakis, E. Psillakis, D. Mantzavinos, Photocatalytic degradation of reactive black 5 in aqueous solutions: Effect of operating conditions and coupling with ultrasound irradiation, Water Res. 41 (2007) 2236–2246.

[37] W. Liu, S. Chen, W. Zhao, S. Zhang, Study on the photocatalytic degradation of trichlorfon in suspension of titanium dioxide, Desalination 249 (2009) 1288–1293.

[38] M.A. Rauf, S. Ashraf, Fundamental principles and application of heterogeneous photocatalytic degradation of dyes in solution, Chem. Eng. J. 151 (2009) 10–18.

[39] Y. Wang, C.S. Hong, Effect of hydrogen peroxide, periodate and persulfate on photocatalysis of 2-chlorobiphenyl in aqueous TiO_2 suspensions, Water Res. 33 (1999) 2031–2036.

[40] I. Poulios, I. Tsachpinis, Photodegradation of the textile dye Reactive Black 5 in the presence of semiconducting oxides, J. Chem. Technol. Biotechnol. 74 (1999) 349–357.

[41] J.M. Herrmann, Heterogeneous photocatalysis: State of the art and present applications In honor of Pr. R.L. Burwell Jr. (1912–2003), Former Head of Ipatieff Laboratories, Northwestern University, Evanston (Ill), Top. Catal. 34 (2005) 49–65.

[42] W. Chu, C.C. Wong, The photocatalytic degradation of dicamba in TiO_2 suspensions with the help of hydrogen peroxide by different near UV irradiations, Water Res. 38 (2004) 1037–1043.

[43] W. Chu, Modeling the quantum yields of herbicide 2,4-D decay in UV/H_2O_2 process, Chemosphere 44 (2001) 935–941.

[44] C.H. Liao, S.F. Kang, F.A. Wu, Hydroxyl radical scavenging role of chloride and bicarbonate ions in the H_2O_2/UV process, Chemosphere 44 (2001) 1193–1200.

[45] R. Yuan, S.N. Ramjaun, Z. Wang, J. Liu, Photocatalytic degradation and chlorination of azo dye in saline wastewater: Kinetics and AOX formation, Chem. Eng. J. 192 (2012) 171–178.

[46] Y. Wang, K. Lu, C. Feng, Influence of inorganic anions and organic additives on photocatalytic degradation of methyl orange with supported polyoxometalates as photocatalyst, J. Rare Earths 31 (2013) 360.

[47] M. Muruganandham, M. Swaminathan, Solar photocatalytic degradation of a reactive azo dye in TiO_2-suspension, Sol. Energy Mater. Sol. Cells 81 (2004) 439–457.

[48] J. Kiwi, A. Lopez, V. Nadtochenko, Mechanism and kinetics of the OH-radical intervention during Fenton oxidation in the presence of a significant amount of radical scavenger (Cl^-), Environ. Sci. Technol. 34 (2000) 2162–2168.

[49] Y. Zhang, R. Selvaraj, M. Sillanpää, Y. Kim, C.W. Tai, The influence of operating parameters on heterogeneous

photocatalytic mineralization of phenol over $BiPO_4$, Chem. Eng. J. 245 (2014) 117–123.

[50] A. Aguedach, S. Brosillon, J. Morvan, E.K. Lhadi, Influence of ionic strength in the adsorption and during photocatalysis of reactive black 5 azo dye on TiO_2 coated on non woven paper with SiO_2 as a binder, J. Hazard. Mater. 150 (2008) 250–256.

[51] M.S. Polo, M.M. Abdel daiem, R.O. Pérez, J.R. Utrilla, A.J. Mota, Comparative study of the photodegradation of bisphenol A by HO, SO_4^- and CO_3^-/HCO_3 radicals in aqueous phase, Sci. Total Environ. 463–464 (2013) 423–431.

[52] N.H. Ince, D.T. Gönenç, Treatability of a textile Azo Dye by UV/H_2O_2, Environ. Technol. 18 (1997) 179–185.